Effects of Physical Confinement on Cancer Cells

Major Qualifying Project

Submitted to the Faculty of

Worcester Polytechnic Institute

In partial fulfilment of the requirements for the

Degree of Bachelor of Science in Physics

By

Mason Miguel

Advised by:

Professor Qi Wen

Abstract

In this report, the biophysical parameters of metastatic MDA-MB-231 and non-carcinoma MCF10a mammary cell lines are collected on 2D hydrogels and in confinement, created *in vitro* by sandwiching cells between two planar hydrogels. Traction force microscopy (TFM) was used to obtain parameters such as traction forces and strain energy, whereas image analysis was used to obtain morphological parameters. Looking at these parameters in tandem can provide insight into how the phenotype or cytoskeletal structure may change in and out of confinement. This paper can provide a better understanding of the metastatic cascade, and thus lay the foundations for future treatments and therapies of cancer.

Table of Contents

Introduction

The Metastatic Cascade

Metastasis, the process by which a secondary tumor is formed in another part of the body, accounts for 90% of all cancer related fatalities. Metastatic cancer cells have several means of escaping the primary tumor site. The most common method is bloodborne dissemination (Eccles & Welch, 2007). Metastatic cells can also spread through lymph nodes, body cavities, or even between the endothelium and basement membrane. Due to the flexibility and complexity of metastatic dissemination, methods of determining the metastatic potential of a tumor, which is the ability for a tumor to form a secondary tumor site, is at the forefront of cancer research.

In order to metastasize via bloodborne dissemination, a cancer cell must detach from the main tumor, and invade into the basement membrane and extracellular matrix (ECM) and enter a nearby blood vessel, called intravasation (Mierke et al., 2008). The invading cell is transported to a secondary site, where the cancer cell will exit the vessel and adhere to the new tissue, called extravasation (Mierke et al., 2008). There are several challenges metastatic cancer cells must overcome in order to form a secondary tumor. To begin, travelling through the collagen-dense ECM may prove difficult (Alcoser et al., 2016). A continuous monolayer of endothelial cells lining the walls of the blood vessel makes intravasation difficult (Hida et al., 2016). While in transit, the cancer cell must avoid immune cells and survive the shear forces present in the blood vessel (Spill et al., 2016). Changes in the tumor microenvironment assist in overcoming these challenges.

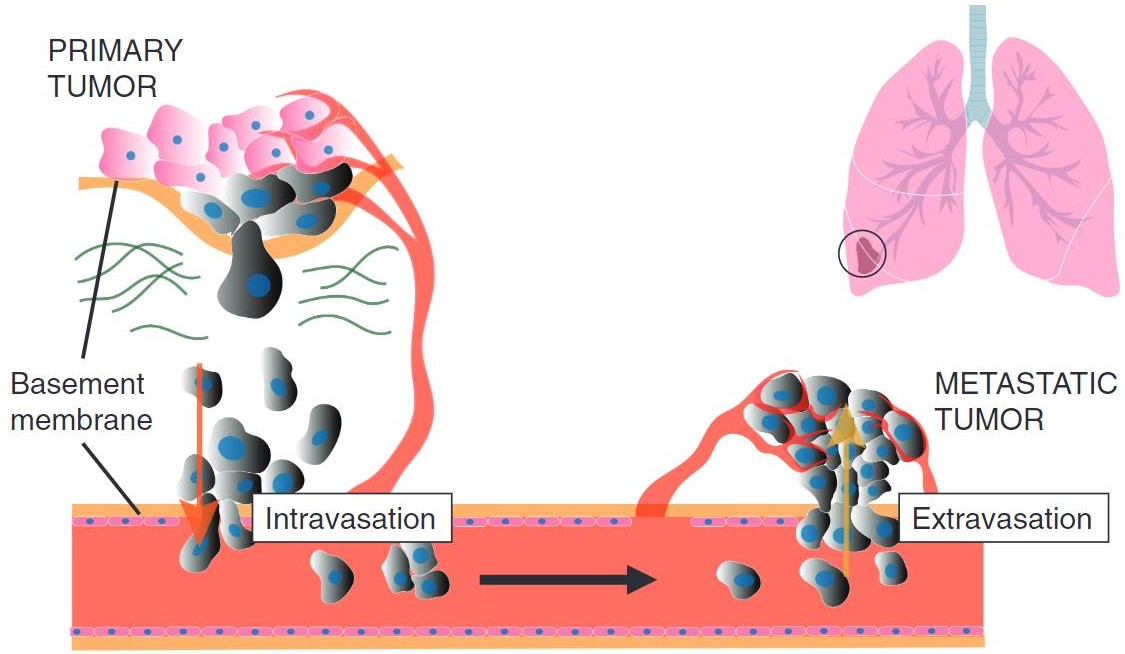

Figure 1: The Metastatic Cascade

Cell Migration Modes

An important aspect of the metastatic process is how invasive cells migrate. Cancer cells can migrate as a collective, connected by cell-cell junctions (Diepenbruck & Christofori, 2016). Invasive cancer cells can take a mesenchymal migration phenotype, characterized by a protruding front end which adheres to the ECM (Wang et al., 2019). Cancer cells can undergo epithelial-mesenchymal transition (EMT), where cells lose their cell-cell contacts and epithelial markers, rearrange their cytoskeleton to have a mesenchymal morphology, and gain mesenchymal markers. Mesenchymal phenotype has a more migratory and invasive behavior, ideal for malignant cells (Diepenbruck & Christofori, 2016). Amoeboid migration is a rapid migration that is more resistant to chemotherapy (Wang et al., 2019). It is energetically favorable and has very little adhesions to the ECM. However, due to the lesser adhesion points as compared to mesenchymal, amoeboid migration does not work in dense ECM. Under the correct conditions, cancer cells can also undergo mesenchymal-amoeboid transition (MAT). For example, cancer affected fibroblasts (CAFs) can remodel ECM proteins and create microtracks for invasive cells to travel through (Alcoser et al., 2016). In these conditions, cells may undergo MAT.

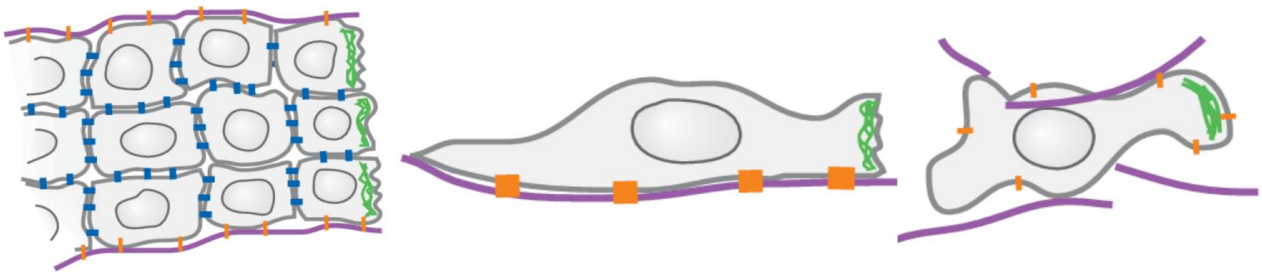

Figure 2: From left to right: Epithelial, mesenchymal and amoeboid migrations

Confinement and the Tumor Microenvironment

When migrating to the blood vessel, invasive cancer cells are under physical confinement: traveling through subnuclear ECM tracks created by cancer affected fibroblasts in addition to intravasating through nanoscopic gaps between endothelial cells lining blood vessels (Alcoser et al., 2015, Chiang et al., 2016, Moiser et al., 2019). Thus, cancer cells under confinement *in vitro* have been studied thoroughly. Using PDMS microchannels, Holle et al. showed that several invasive cancer cell lines change their migratory phenotype under physical confinement (Holle et al., 2019). In this study, it was found that in confining channels (with widths from 3-10μm) metastatic cells change from mesenchymal focal adhesion migration to amoeboid migration, undergoing MAT. Moreover, Mosier et al. found that for varying levels of confinement, metastatic breast cancer cells react differently: altering the size and density of adhesion sites, traction forces and migration speed (Moiser et al., 2019). Similarly, this study also found amoeboid migration triggered by full confinement.

The tumor microenvironment can be defined as the cancer-affected and unaffected cells in and around the tumor. The tumor microenvironment sees several biophysical changes during tumorigenesis (Spill et al., 2016). These biophysical changes can then affect the behavior in certain cell population behaviors. For instance, tumors must form new blood vessels in order to grow and receive nutrients, a process called angiogenesis. These tumor-formed vessels have abnormalities that create gaps in the endothelial monolayer and allow for invading cells to enter the blood stream easier (Hida et al., 2022).

The tumor microenvironment is recreated in vitro using several methods. Microfluidic polydimethylsiloxane (PDMS) devices are often used to model cell intravasation and extravasation as microchannels can be formed within them with widths of several microns using

lithography techniques (Amos & Choi, 2021). However, PDMS is not the ideal platform for experiment, as its stiffness in range of several MPa greatly exceeds that of human tissue, which typically goes up to 20 kPa (Wang et al., 2019). For experiments where substrate stiffness is important, a hydrogel is preferred (Amos & Choi, 2021). 3D hydrogel experiments can be used to study cell-cell and cell-ECM interactions, such as ECM remodeling (Alcoser et al., 2016). For single cell experiments where these interactions are not important, 2D hydrogel is preferred. A 2D hydrogel provides an idealized environment to study single cell morphologies and traction forces.

Cellular Traction Forces

A cell's traction forces are also altered during tumor development, caused by the increased stiffness of the ECM (Wang, 2010). Cell traction forces are used by cells for fundamental functions such as ECM reorganization, communication, and migration (Wang, 2010). As such, quantifying cell traction forces could be deeply important for metastasis research. For example, Alcoser et al. found that tissue-isolated cancer-associated fibroblasts exerted 50% greater traction forces than their normal counterparts (Alcoser et al., 2016). In addition, because metastatic cells must travel through physically confined spaces during intravasation and extravasation, it is important to understand how these cell traction forces change while under physical confinement.

Traction force microscopy (TFM) is a method of quantifying the cellular forces exerted on a substrate. The substrate has fluorescent nanoparticles evenly distributed on its surface that are used to determine small displacements. Cells will then be plated on the substrate, and they will exert traction forces on the gel surface. The bead positions can then be observed without any traction forces by detaching the cells. Traction fields can be generated using the bead positions before and after detachment (Schwarz & Soine, 2015). The substrate is typically coated in collagen or fibronectin, to allow for actin of the cytoskeleton to adhere to a surface. The gel is typically a polyacrylamide (PA) gel, as the stiffness of the gel can be modified to fit within the typical stiffness of human tissue (0.1 – 20kPa) (Wang et al., 2019).

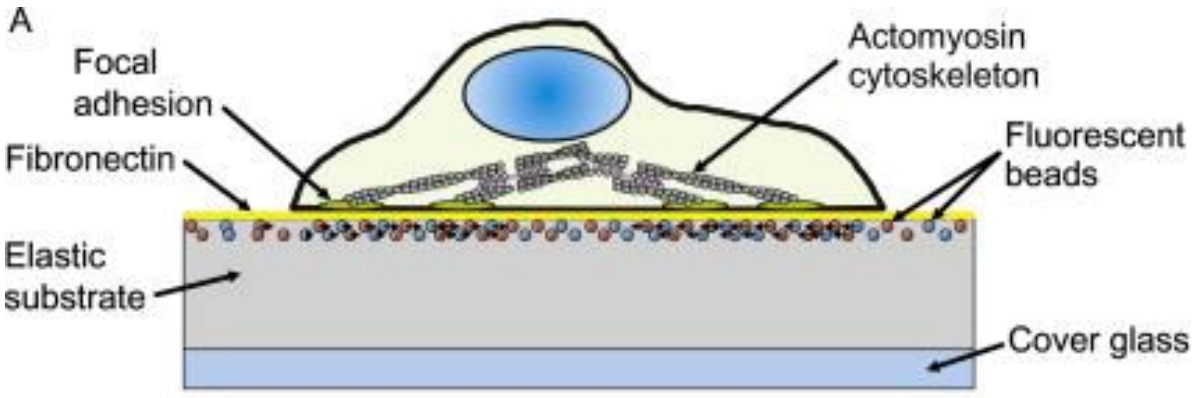

Figure 3: Diagram for Traction Force Microscopy

In vivo, cells experience varying degrees of physical confinement. Further, metastatic cells are under great confinement during intravasation and extravasation. Thus, it is important to study how confinement changes cell behavior. From previous studies, it has been shown that confinement can change the phenotype, morphology, and adhesive forces of a cell line (Alcoser et al., 2016; Moiser et al., 2019). For example, Shen et al. found that physical confinement of glioblastoma (G55) and breast cancer (MDA-MB-231) cell lines induce resistance to cancer treatment (Shen et al., 2021). Moreover, it has been shown that physical confinement can affect the traction forces of neutrophils (Toyjanova et al., 2015).

In this paper, the traction forces and morphology data will be collected for MDA-MB-231 breast cancer and MCF10a breast epithelial cell lines on a 2D hydrogel. This data will be compared to the traction forces and morphology of the same cell lines under confinement. The confinement method used has been called 2.5D in the literature (Toyjanova et al., 2015). This data can provide insight into how cancer cells adapt to the novel environments seen during the metastatic cascade. This can then be used for new methods of treatments and therapy.

Methods and Materials

Gel Preparation

For TFM and morphology experiments, cells were plated onto polyacrylamide (PAA) hydrogels. Since the typical range of human tissue can range up to 20 kPa, three hydrogel stiffness were used: 3.2 kPa, 7.5 kPa and 20 kPa (Wang et al., 2019). In order to track gel displacements from cell adhesions, 0.1µm fluorescent beads, 300x diluted were used. Plasma treated 18mm round coverslips were used to set the hydrogel and ensure a planar surface. 17 µL of bead solution was pipetted onto the treated coverslip and was spun on a spinner at 6000 RPM, and then the process was repeated a second time. Spinning, in addition to sonicating the bead solution, ensures an ideal distribution of beads and reduces the number of aggregated beads.

Once the coverslips were treated with beads, a hydrogel solution was prepared. Depending on the desired stiffness, concentrations of acrylamide and bisacrylamide were mixed with HEPES (See Table 1). 10 µL of Ammonium Persulfate (APS) and 3 µl of TEMED were added in order to initiate polymerization of the gel. 25 µl of the gel solution was pipetted onto the treated coverslips and is attached to a glutaraldehyde treated glass slide. The gel was left to fully polymerize (about 15 minutes), sealed in parafilm, soaked in HEPES, and stored.

Condition	HEPES (µL)	ACL (µL)	Bis (µL)
3.2 kPa	815	125	60
7.5 kPa	750	200	50
20 kPa	630	300	70

Table 1: The hydrogel stiffness used in this paper and measures of HEPES, ACL, and Bis needed

Prior to cell plating, a collagen coating is needed so that the cells can adhere to the gel. 200 µL of crosslinker sulfo-SANPAH was added to the surface of the gel. The gel was then UV treated, allowing the sulfo-SANPAH to bond to the gel surface. Once bonded, the gel is washed three times with HEPES. A 0.1 mg/mL collagen-PBS solution is made, and 1 mL is added to each plate. The dishes are left at room temperature for 3-4 hours to allow the collagen to adhere to the sulfo-SANPAH.

Cell Preparation

MDA-MB-231 breast cancer and MCF10a breast epithelial cell lines were used in this experiment, provided by Wen Lab. MDA-MB-231 were cultured in Dulbecco's Modified Eagle Medium (DMEM), supplemented with 10% fetal bovine serum (FBS) and L-Glutamine. MCF10a was cultured in DMEM supplemented with 1% penicillin-streptomycin, 5% horse serum, 1% hydrocortisone, 0.1% insulin, 0.1% cholera toxin, and 0.02% epidermal growth factor (EGF). Cells are seeded onto the gel when the culture plate reaches a confluency between 80-90%.

After collagen is adhered to the gel, it is washed three times with PBS. 500 µl of cell media is added to the gel and left in the incubator for 30 minutes. This allows the gel to absorb the media and warm the gel to the proper temperature for the cells. Afterwards, cells are plated onto the gel in a concentration of 25,000 cells/ml. The cells are allowed to fully adhere to the hydrogel for 24 hours

Confinement

For confinement experiments, a hydrogel is prepared in a similar process previously described, only no beads are treated to the gel, and no collagen is bonded to the surface. This gel is washed three times with PBS and allowed to soak in media for 30 minutes. Cells that have had 24 hours to adhere to the bottom gel are then sandwiched by this secondary gel. To ensure the top hydrogel does not float, a polydimethylsiloxane (PDMS) weight of approximately 1g is attached to the top gel. After an additional 24 hours, the plate is ready for experimentation.

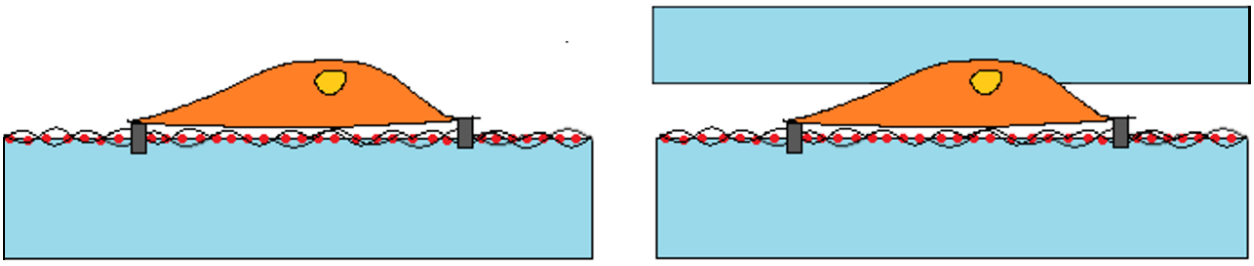

Figure 4: The experimental diagram for the unconfined experiment (left) and the confined experiment (right)

Traction Force and Morphology Experiments

TFM experiments were conducted using an Olympus IX83 microscope on a 40x objective and acquired using a CCD camera. The beads were excited, and in turn the beads fluoresced in the red fluorescent protein (RFP) wavelength. For each cell, an image was taken of the cell in phase contrast, and then two captures were taken of the RFP, one before cell detachment, and one after; cells were detached using trypsin. Bead displacement vectors were constructed using MATLAB, and ANSYS was used to calculate the traction forces generated by the cell. Morphology experiments were conducted using the same equipment as the TFM experiment. Cells were seeded at a much higher concentration of about 100,000 cells/ml. Images were taken in phase contrast. Data analysis was performed using ImageJ where cell area, circularity and aspect ratio of the cell was recorded.

Results

Cells React to Varying Substrate Stiffness

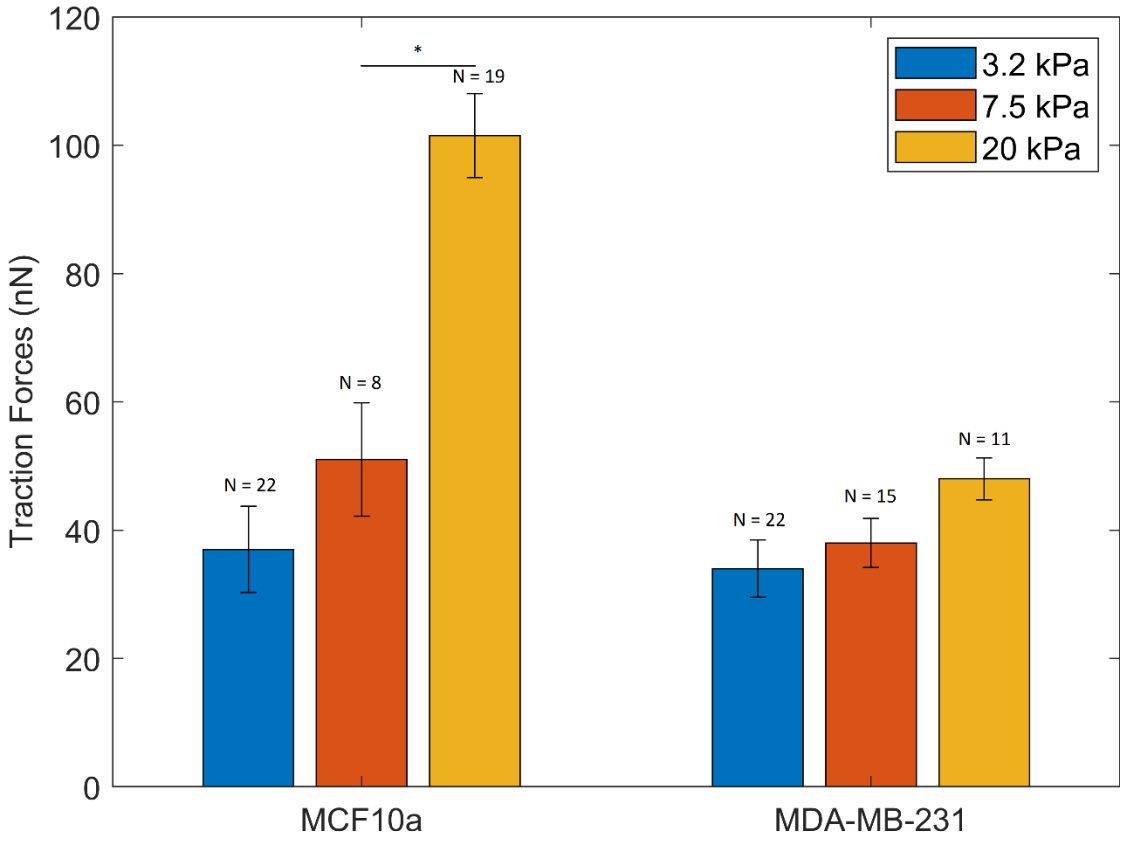

Figure 5: The traction forces of MCF10a and MDA-MB-231 cell lines on the 3.2 kPa, 7.5 kPa and 20 kPa gels

First, MDA-MB-231 and MCF10a cell lines were plated on a 2D hydrogel without confinement. Three levels of stiffness were used: 3.2 kPa, 7.5 kPa and 20 kPa. These stiffnesses are within human tissue range of stiffnesses. As expected, for both cell lines the traction forces increase with gel stiffness. For the MDA-MB-231 cells, though the means of each condition increase with substrate stiffness, there is no significant difference from condition to condition. It appears the MCF10a cells have a greater reaction to stiffness than the MDA-MB-231 cell lines. There is some significant difference between the 7.5 kPa and 20 kPa conditions, but no significant difference between the 3.2 kPa and 7.5 kPa conditions. Figure 5 shows cells from each condition and their traction forces. It is expected that both the MDA-MB-231 and MCF10a cell lines would have a similar morphology to their in-culture morphology. MDA-MB-231 cells have an elongated morphology, with many protrusions and adhesion points. On the other hand, MCF10a cells exhibit a more rounded shape, with a higher circularity and more lamellipodial adhesions. From the unconfined experiments, both MCF10a cells and MDA-MB-231 cells take their expected morphology.

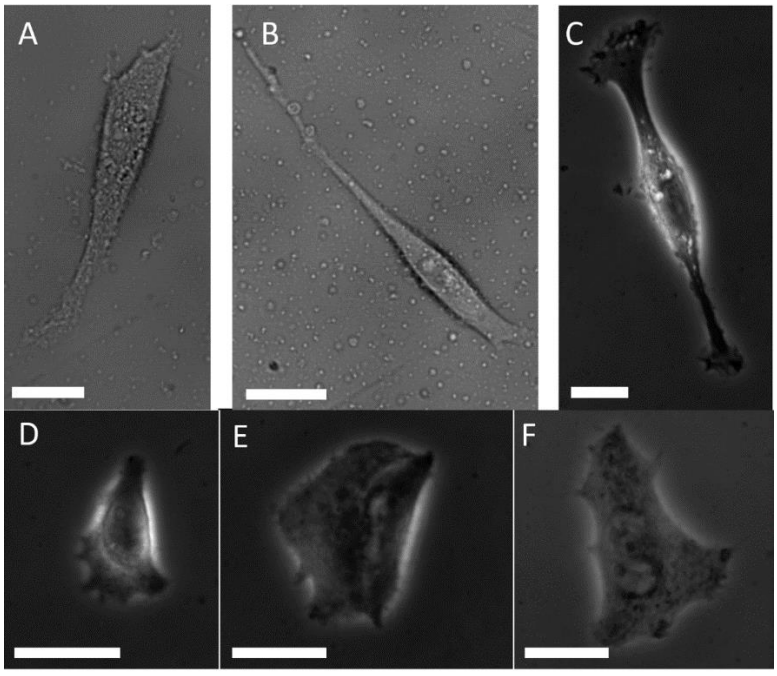

Figure 6: Phase contrast images of MDA-MB-231 and MCF10a cells on 3.2 kPa gel (A, D), 7.5 kPa gel (B, E), and 20 kPa gel (C, F), respectively. Scale bar: 10 µm

Different Reactions to Confinement Between the Two Cell Lines

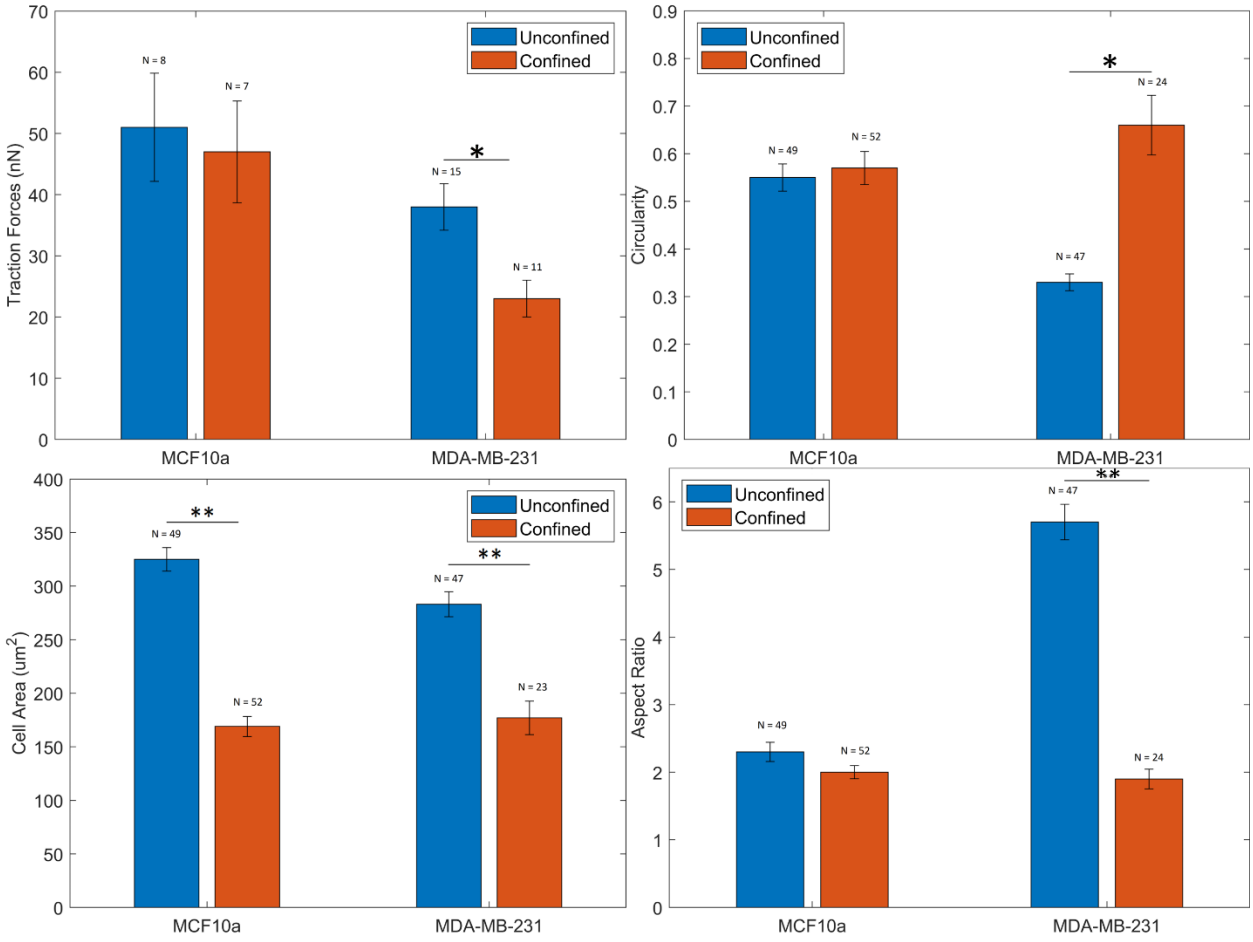

Figure 7: The traction forces (top left), cell area (top right), circularity (bottom left) and aspect ratio (bottom right) of MCF10a and MDA-MB-231 cells in and out of confinement

For the experiments under confinement, 7.5 kPa gels were used for both the top confining and bottom gels. For the MCF10a cell line, there was no significant change between the confined and unconfined condition. For the MDA-MB-231 cell line, there was a significant decrease from the unconfined to the confined condition. Thus, the two cell lines seem to react to confinement differently. In order to further understand the difference in reactions to confinement, the morphology of both cell lines was analyzed. More specifically, the cell area, circularity, and aspect ratio (AR) were analyzed.

Once again, different reactions were found in and out of confinement for the cell lines. For both cell lines, a significant decrease in area was found from unconfinement to confinement.

This is expected, as confinement applies additional force onto the cell. Looking at the circularity, there is no significant change for MCF10a samples, but a significant increase for MDA-MB-231 samples. Similarly, for AR, there is no significant change for MCF10a cells, but a significant decrease for MDA-MB-231 cells. An increase in circularity and decrease in AR tells us that the MDA-MB-231 cells are taking a less spindly, more rounded morphology with less adhesion points.

MDA-MB-231 are More Energy Efficient Under Confinement

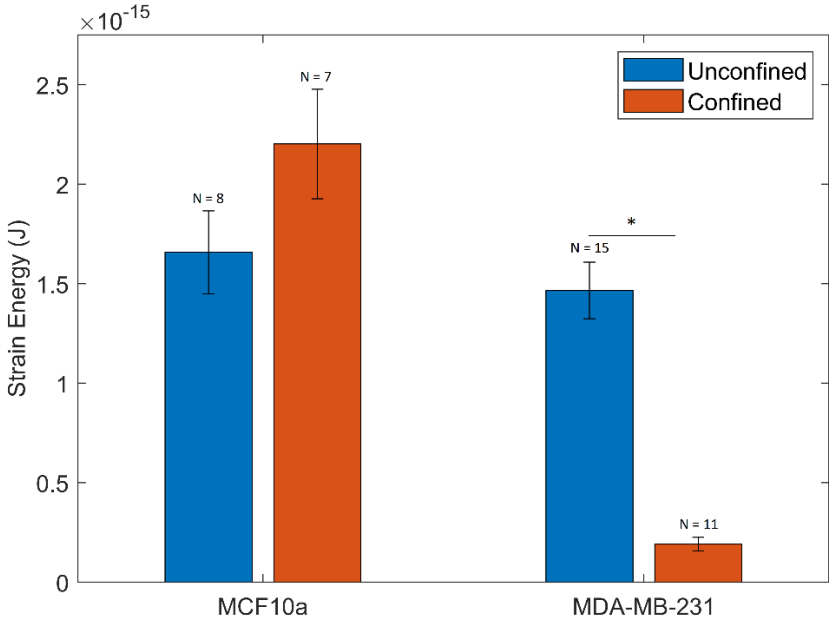

Figure 8: The strain energy for MCF10a cells and MDA-MB-231 Cells in and out of confinement

The analysis of strain energy provides further insights into the underlying mechanisms of cellular behavior. Strain energy is an important parameter that tells us the overall energy exerted by the cells onto the substrate. For the MCF10a cell line, there is no significant change to their stress energy when entering confinement. However, for the MDA-MB-231 cell line, there was a significant decrease in the energy exerted under confinement. This suggests that the metastatic cells are in some way more energy efficient when confined than the non-carcinoma cells.

Discussion

The results of the experiments in and out of confinement provide valuable insights into the response of the metastatic cell line, MDA-MB-231, and non-metastatic cell line, MCF10a.

From these experiments, it was shown that MCF10a did not have significant changes to circularity, aspect ratio or traction forces when subjected to confinement. On the other hand, MDA-MB-231 did exhibit statistically significant changes to these parameters. This could indicate that MDA-MB-231 cells transitioned from a mesenchymal morphology to a more amoeboid morphology in response to confinement.

Amoeboid morphology is characterized by a lack of adhesion points and lamellipodia, a more rounded shape, and a proven resistance to chemotherapy. Additionally, because they lack well-defined adhesion points, amoeboid cells can detach and reattach to substrates quickly, enabling them to rapidly change direction or adapt to changes in their environment (Wang et al., 2019). Given that MDA-MB-231 cells exhibited reduced traction forces, greater circularity, and reduced aspect ratio when under confinement, it is reasonable to suggest that this cell line may have transitioned to amoeboid morphology. Figure 7 compares phase contrast images of MDA-MB-231 cells in and out of confinement to mesenchymal and amoeboid diagrams. The differences in morphology are clearly visible: the unconfined MDA-MB-231 cell has clearly visible adhesion points, whereas the confined MDA-MB-231 cell has no visible adhesion points.

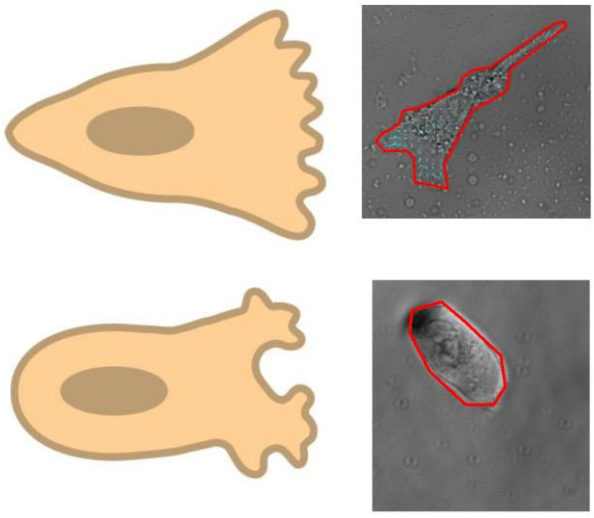

Figure 9: Diagrams of mesenchymal (top left) and amoeboid (bottom left) morphologies and phase contrast images of MDA-MB-231 cells unconfined (top right) and confined (bottom right)

Previous experiments also have shown that confinement can have effects on the morphology and traction forces of a cell line. For example, Wang et al. explored the synergistic effect of confinement and substrate stiffness on cell morphology. For some levels of substrate

stiffness, increasing the degree of confinement led to changes in morphology, where greater confinement corresponded to cells taking an amoeboid morphology. Furthermore, Holle et al. showed that several invasive cancer cell lines change their migratory phenotype under physical confinement (Holle et al., 2019).

Conclusion

In conclusion, the results of these experiments highlight the differential response of MDA-MB-231 and MCF10a cell lines to confinement. The MCF10a cells did not show significant changes in their morphology and traction forces when subjected to confinement, while the MDA-MB-231 cells exhibited a transition from a mesenchymal morphology to an amoeboid morphology. This transition could have important implications for the cells' invasive behavior, as amoeboid cells are known to have a higher degree of motility, invasiveness, and resistance. Overall, these findings provide insights into the cellular response to confinement and have the potential to inform new strategies for cancer treatment and drug development.

Future directions

Metastasis is a complicated subject, and by extension so are the effects of physical confinement. As such, it would be impossible to fully understand how confinement affects cancer cell mechanics with just one experiment. For future directions of this project, I recommend exploring varying degrees of confinement by increasing or decreasing the distance between the bottom gel and its confining top gel. This can be achieved using a micromanipulator, which can have an accuracy within a few microns. Previous literature, such as Wang et al., have shown that varying degrees of confinement can have varying effects on a cell’s mechanics.

Further, it will also be important to recreate the confinement cells are subjected to during metastasis more accurately. Thus, future experiments can explore confinement where both top and bottom gels are treated with collagen, or some other ECM ligand. Moreover, it will be important to explore the effects of confinement over a period of time. Lastly, it will also be important to study the biochemical effects of confinement in addition to the biophysical. Western blots can provide insight into how the chemical makeup of cells change due to confinement and using inhibitors such as Arp 2/3 inhibitor CK-666 can provide insight into which compounds are

initiating change in the cell's morphology. Only through rigorous experimentation will scientists be able to better understand the metastatic cascade, and thus be able to devise new treatments and therapies.

Acknowledgements

I would like to thank my advisor, Professor Qi Wen, for his support and guidance on my project, in addition to allowing me access to his laboratory resources. Further, I would also like to thank graduate students Theadora Vassella, Pengbo Wang and Jiazhang Chen, who taught me the laboratory skills necessary for my project. Lastly, I would like to thank Worcester Polytechnic Institute's Physics Department, without whom this MQP would not be possible.

References

Alcoser, T. A., Bordeleau, F., Carey, S. P., Lampi, M. C., Kowal, D. R., Somasegar, S., Varma, S., Shin, S. J., Reinhart-King, C. A. (2015). Probing the biophysical properties of primary breast tumor-derived fibroblasts. *Cellular and Molecular Bioengineering*, 8(1), 76-85.

Amos, S., Choi, Y. (2021) The cancer microenvironment: mechanical challenges of the metastatic cascade. *Frontiers in Bioengineering and Biotechnology* 9(1).

Chiang, S., Cabrera, R., Segall, J. (2016) Tumor cell intravasation. *American Journal of Physiology* 311(1) C1-C14.

de Vicente, G., Lensen, M. (2016). Topographically and elastically micropatterned PEG-based hydrogels to control cell adhesion and migration. *European Polymer Journal*, 78(1) 290-301.

Diepenbruck, M., Christofori, G. (2016) Epithelial–mesenchymal transition (EMT) and metastasis: yes, no, maybe. *Current opinion in Cell Biology*, 43(1) 7-13.

Eccles, S. A., & Welch, D. R. (2007). Metastasis: recent discoveries and novel treatment strategies. *Lancet*, 369(1), 1742-1757.

Hida, K., Maishi, N., Takeda, R., Hida, Y. (2022) The roles of tumor endothelial cells in cancer metastasis. *Metastasis*. Brisbane (AU): Exon Publications. Online first 2022 Mar 13.

Hida, K., Maishi, N., Torii, C., Hida, Y. (2016) Tumor angiogenesis—characteristics of tumor endothelial cells. *International Journal of Clinical Oncology*, 21(1), 206-212.

Holle, A., Devi, N., Clar, K., Fan, A., Saif, T., Kemkemer, R., Spatz, J. (2019) Cancer Cells Invade Confined Microchannels via a Self-Directed Mesenchymal-to-Amoeboid Transition. *Nano Letters*, 19(4) 2280-2290

Mierke, C. T., Rösel D., Fabry, B., Brábek, J. (2008) Contractile forces in tumor cell migration. *European Journal of Cell Biology*, 87(1), 669-676.

Moiser, J., Rahman-Zaman, A., Zanotelli, M., VanderBurgh, J., Bordeleau, F., Hoffman, B., Reinhart-King, C. (2019) Extent of Cell Confinement in Microtracks Affects Speed and Results in Differential Matrix Strains. *Biophysical Journal* 117(9) 1692-1701.

Spill, F., Reynolds, D. S., Kamm, R. D., & Zaman, M. H. (2016). Impact of the physical microenvironment on tumor progression and metastasis. *Current Opinion in Biotechnology*, 40(1), 41-48.

Wang, J. H. (2010). Cell Traction Forces (CTFs) and CTF Microscopy Applications in Musculoskeletal Research. *Operative Techniques in Orthopaedics*, 20(2), 106-109.

Wang, M., Cheng, B., Yang, Y., Liu, H., Huang, G., Han, L., Li, F., Xu, F. (2019). Microchannel Stiffness and Confinement Jointly Induce the Mesenchymal-Amoeboid Transition of Cancer Cell Migration. *Nano Letters*, 19(1), 5949-5958.

Schwarz, U. S., Soine, J. R. (2015). Traction force microscopy on soft elastic substrates: A guide to recent computational advances. *BBA – Molecular Cell Research*, 1853(11B) 3095-3104.

Shen, Q., Hill, T., Cai, X., Bui, L., Barakat, R., Hills, E., Almugaiteeb, T., Babu, A., Mckernan, P., Zalles, M., Battiste, J. (2021). Physical confinement during cancer cell migration triggers therapeutic resistance and cancer stem cell-like behavior. Cancer Letters, 506(1) 142-151.

Tiwari, N., Gheldof, A., Tatari, M., Christofori, G. (2012) EMT as the ultimate survival mechanism of cancer cells. *Seminars in Cancer Biology*, 22(3), 194-207.

Toyjanova, J., Flores-Cortez, E., Reichner, J., Franck, C. (2015). Matrix Confinement Plays a Pivotal Role in Regulating Neutrophil-generated Tractions, Speed, and Integrin Utilization. *Journal of Biological Chemistry*, 290(6) 3752-3763